Available online at www.sciencedirect.com

SCIENCE DIRECT

Surface & Coatings Technology 199 (2005) 22 – 31

SURFACE & COATINGS TECHNOLOGY

www.elsevier.com/locate/surfcoat

TiO_2 coating for long-cycling $LiCoO_2$: A comparison of coating procedures

George Ting-Kuo Fey[a,*], Cheng-Zhang Lu[a], T. Prem Kumar[a,1], Yu-Chen Chang[b]

[a]Department of Chemical and Materials Engineering, National Central University, Chung-Li, 32054 Taiwan, ROC
[b]Department of Chemical Engineering, Yuan Ze University, Taoyuan, Nelli, Taiwan 301, Taiwan, ROC

Received 4 November 2003; accepted in revised form 17 March 2005
Available online 12 May 2005

Abstract

The cycling properties of $LiCoO_2$ coated with TiO_2 by a sol–gel process from an alkoxide precursor and a mechano-thermal process from pre-formed nanoparticles are compared. Electron microscopic images of 1.0 wt.% TiO_2-coated particles revealed that the oxide formed a compact coating over the cathode particles. XRD studies showed a general decrease in the value of the lattice parameter *c* upon coating, indicating that substitutional compounds might have formed on the surface during calcination. *R*-factor values from XRD studies and galvanostatic charge–discharge studies suggested that a coating level of 1.0 wt.% was optimal for materials with good cycling characteristics. While the sol–gel coating process enhanced cyclability 5-fold, the mechano-thermal process yielded materials that exhibited a 12-fold improvement. The enhanced cyclability is attributed to a suppression of the cycle-limiting hexagonal/monoclinic/hexagonal phase transitions accompanying the charge–discharge processes. Materials with better electrochemical characteristics could be obtained by the mechano-thermally coating process than sol–gel. Furthermore, the mechano-thermal coating process is a simple, inexpensive, environmentally benign and commercially viable one for the production of high-cycling $LiCoO_2$ cathode materials.

Keywords: Coated cathodes; Sol–gel coating; Mechano-thermal coating; Coated $LiCoO_2$; Nanoparticles; Lithium-ion battery

1. Introduction

Crystalline $LiCoO_2$ is the most widely investigated cathode material for lithium rechargeable batteries due to its high energy density and relatively good cycling performance. $LiCoO_2$ has a hexagonal α-$NaFeO_2$ structure in which the cobalt ions reside in octahedral interstitial sites in a cubic closely packed array of oxygen atoms in such a way that the CoO_2 layers are formed by edge-sharing $[CoO_6]$ octahedra. The lithium ions are present in octahedral $[LiO_6]$ coordination between the CoO_2 layers. Repeated cycling of this material results in a loss in capacity, especially if the charging voltages exceed 4.2 V. The capacity fade is attributed to anisotropic expansion and contraction of the lattice during cycling [1–7]. Delithiation of $LiCoO_2$ is accompanied by an expansion of the host lattice in the *c*-direction, as a result of the increased electrostatic repulsion between adjacent oxygen layers [8,9], and a contraction in the Co–Co distance [1,2]. Restricting the charging voltage to 4.2 V leads to the cycling of only 0.5 Li per molecule, which translates to a charge density of about 140 mA h/g.

An additional factor responsible for the degradation of the cathode is believed to be the dissolution of tetravalent cobalt from the active particles [10]. It has been suggested that the electrochemical behavior of cathode-active materials is strongly dependent on the surface chemistry of the cathode [10,11]. The dissolution of Co^{4+} would not only mean a loss of active material, but also the introduction of inactive phases in the cathode [12].

One approach adopted to enhance the cyclability of cathode materials is to coat the cathode particles with an oxide such as Al_2O_3 [4–6,13,14], B_2O_3 [6], MgO

* Corresponding author. Tel.: +886 3 425 7325 or +886 3 422 7151x34206; fax: +886 3 425 7325.
E-mail address: gfey@cc.ncu.edu.tw (G. Ting-Kuo Fey).
[1] On deputation from: Central Electrochemical Research Institute, Karaikudi 630 006, TN, India.

0257-8972/$ - see front matter © 2005 Elsevier B.V. All rights reserved.
doi:10.1016/j.surfcoat.2005.03.021

[12,15,16], SnO_2 [17], TiO_2 [6,14] and ZrO_2 [6,14]. Some authors suggest that the coating materials form substitutional oxides on the cathode surface, which bestow improved structural stability to the core material and enhance its cyclability [15,17]. Cho et al. [6] suggest that the coatings with high fracture-tough materials suppress the cycle-limiting phase transitions associated with the intercalation–deintercalation processes. Additionally, the presence of an inert oxide coating on the cathode particle can limit the direct contact of the active material with the electrolyte, and thus prevent dissolution of cobalt in the electrolyte [12,18].

The coating procedures adopted in the above studies were based on the sol–gel or precipitation technique, in which the oxide formed by the hydrolysis of a metal compound such as an alkoxide was deposited in situ, followed by a calcination step. Recently, we demonstrated a simple and economical mechano-thermal process by which pre-formed nanoparticles of fumed silica [19], pseudo-boehmite [20] and boehmite [21] were deposited on commercial $LiCoO_2$ powders. The cyclability of such coated particles improved several fold. Although the sol–gel coating process also yields cathodes with improved cyclability, it is beset with problems such as the high cost of alkoxide precursors and the release of environmentally hazardous alcoholic by-products, which make the procedure's commercial applicability questionable. Thus, the mechano-thermal coating process can be a convenient alternative to the conventional sol–gel/precipitation coating processes. In this paper, we compare the sol–gel and mechano-thermal processes for the production of TiO_2-coated $LiCoO_2$ with extended cyclability.

2. Experimental

2.1. TiO_2 coating

$LiCoO_2$ powder, with an average particle size 1–8 μm, was a commercial product of Coremax Taiwan Corporation. The sol–gel coating with TiO_2 was adopted from the polymeric precursor method described by Bianco et al. [22]. Briefly, titanium tetrabutoxide, 0.0255 g, 0.0852 g, and 0.2556 g, was added to a 60:40 mixture of ethylene glycol and citric acid and sonicated with 2 g $LiCoO_2$ for 30 min, such that the ratios of $LiCoO_2$ to the TiO_2 obtainable from the precursor were 99.7:0.3, 99.0:1.0 and 97.0:3.0, respectively. This mixture was warmed at 120 °C to obtain a gel with dispersed $LiCoO_2$ particles, which was subsequently dried in an air oven at 120 °C. The resulting suspension of $LiCoO_2$ in the polymeric precursor was initially heated at 300 °C, and finally calcined at 750 °C for 10 h.

The mechano-thermal coating was performed as follows. A weighed amount of TiO_2 (P25 sample from Degussa AG, particle size: 21 nm) was dispersed in ethanol by a 1-h sonication followed by 10 h of vigorous stirring. $LiCoO_2$ was added to this dispersion such that the weight ratios of TiO_2 to the cathode material were 0.3:99.7, 1.0:99.0 and 3.0:97.0. The mixture was sonicated for 30 min, and stirred on a magnetic stirrer for 24 h. A subsequent slow evaporation of the solvent at 50 °C resulted in a black dry mass of TiO_2-coated $LiCoO_2$ particles. The coated particles were calcined at 450 °C for 10 h in order to ensure good adhesion of the coated particles with the core material.

2.2. Structural and morphological characterization

An X-ray diffractometer (XRD) (Siemens D-5000, Mac Science MXP1) equipped with a nickel-filtered Cu-K_α radiation source was used for structural analysis. The diffraction patterns were recorded between scattering angles of 5° and 80° in steps of 0.05°. Brunauer–Emmett–Teller (BET) surface area measurements were carried out on a Micromeritics ASAP 2010 surface area analyzer. The surface morphological studies were carried out on a scanning electron microscope (Hitachi model S-3500V). The microstructures of the coated particles were examined by a JEOL JEM-4000EX high-resolution transmission electron microscope (HRTEM). The samples for HRTEM studies were prepared by dispersing the coated powders in ethanol, placing a drop of the clear solution on a carbon-coated copper grid, and subsequent drying. Depth profiles of titanium, cobalt and oxygen in the coated materials were recorded by an electron spectroscopy for chemical analysis (ESCA) (VG Scientific ESCALAB 250) in order to analyze the spatial distribution of the ions in the cathode particles.

2.3. Electrochemical characterization

Coin cells of the 2032 configuration were assembled in an argon-filled VAC MO40-1 glove box in which the oxygen and water contents were maintained below 2 ppm. Lithium metal (Foote Mineral) was used as the anode and a 1 M solution of $LiPF_6$ in EC:DEC (1:1 v/v) (Tomiyama Chemicals) was used as the electrolyte. The cathode was prepared by blade-coating a slurry of 85 wt.% coated active material with 10 wt.% conductive carbon black and 5 wt.% poly(vinylidene fluoride) binder in *N*-methyl-2-pyrrolidone on an aluminum foil, drying overnight at 120 °C in an oven, roller-pressing the dried coated foil, and punching out circular discs. The cells were cycled at a 0.2 C rate (with respect to a theoretical capacity of 274 mA h/g) between 2.75 and 4.40 V in a multi-channel battery tester (Maccor 4000). Phase transitions occurring during the cycling processes were examined by a slow scan cyclic voltammetric experiment, performed with a three-electrode glass cell. The working electrodes were prepared with the cathode powders as described above, but coated on both sides of the aluminum foil. The cells for the cyclic voltammetric studies were assembled inside the glove box with lithium metal foil serving as both counter and reference electrodes. The electrolyte used was the same as that for the coin cell.

Cyclic voltammograms were run on a Solartron 1287 Electrochemical Interface at a scan rate of 0.025 mV/s between 3.0 and 4.4 V.

3. Results and discussion

3.1. X-ray diffraction

The diffraction patterns of $LiCoO_2$ coated with different amounts of sol–gel derived TiO_2 are compared with those of bare $LiCoO_2$ in Fig. 1, while those of the mechano-thermally coated materials are shown in Fig. 2. The diffraction patterns conform to the $R\bar{3}m$ symmetry of the core material. The fact that no diffraction patterns corresponding to the coating material were observed is expected since it existed as a thin film and possibly as a mixed oxide formed by interaction with the core material. Table 1 shows that the lattice constants c of the coated materials were generally less than those of the bare sample, suggesting that the phases on the surface of the powder were solid solutions formed by the reaction of the TiO_2 particles with the core material. It is possible that during the 10 h calcination process, a substitutional compound of the composition $LiTi_yCo_{1-y}O_{2+0.5y}$ could have formed through the interaction of the coated oxide with the substrate. The general contraction in the c parameter may indicate such a possibility, although it must be noted that the crystal ionic radius of Ti^{4+} (0.745 Å) is larger than that of Co^{3+} (0.545 Å). Similar inter-oxide surface compositions have also been proposed by other researchers [4,12,15,23]. Cho et al. [17] speculate that nominally pure $LiCoO_2$ is defective and contains a small fraction of Co^{4+}, which could be compensated for by vacancies in the cobalt sublattices. According to these authors [17], the substitution of a tetravalent ion is possible in the interstitial Co^{4+} sites. Thus, we expect the formation of an inter-oxide surface film of composition $LiTi_yCo_{1-y}O_{2+0.5y}$.

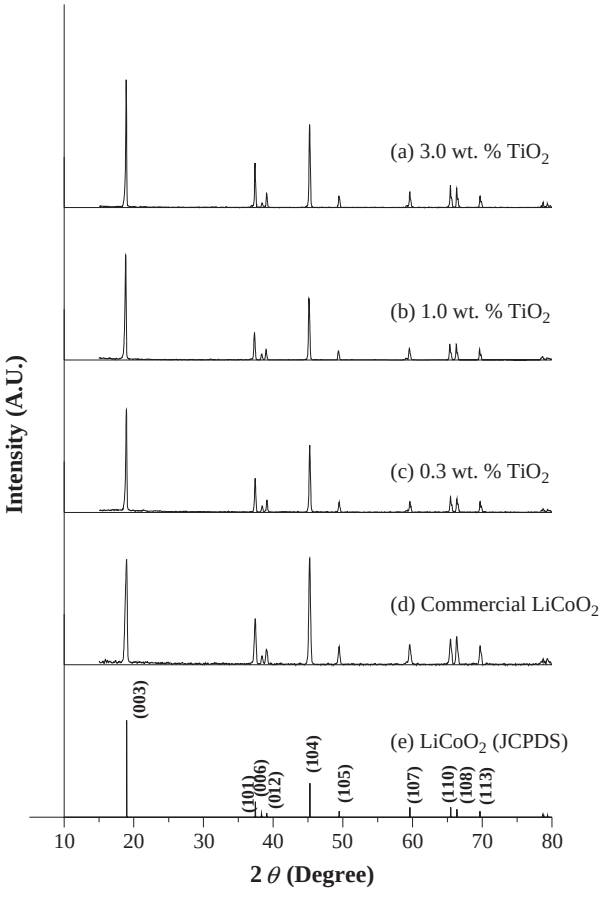

Fig. 1. Powder X-ray diffraction patterns of $LiCoO_2$ coated with TiO_2 by the sol–gel method.

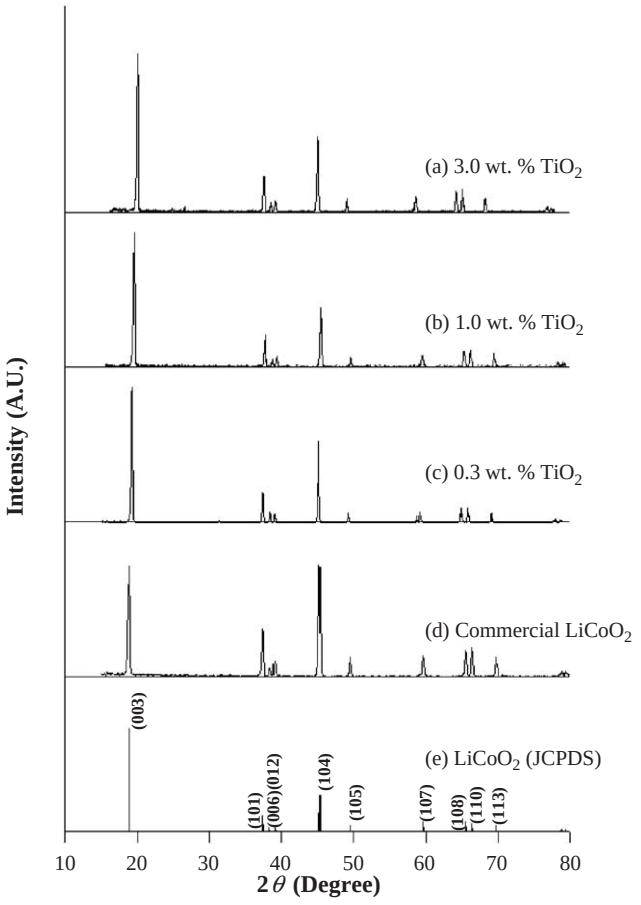

Fig. 2. Powder X-ray diffraction patterns of $LiCoO_2$ coated with TiO_2 by the mechano-thermal process.

According to Dahn et al. [24,25], the R-factor, defined as the ratio of the intensities of the hexagonal characteristic doublet peaks (006) and (012) to the (101) peak, is an indicator of hexagonal ordering: the lower the R-factor, the better the hexagonal ordering and, hence, the electrochemical performance. The values of the R-factor for the sol–gel coated samples are given in Table 1. It can be seen that the R-value was the lowest at the 1.0 wt.% coating level. Similarly, among the mechano-thermally coated samples, the 1.0 wt.% TiO_2-coated material had the lowest R-value (Table 1). As we will see below, the electrochemical

Table 1
Lattice parameters and *R*-factor values of the bare and TiO_2-coated $LiCoO_2$

Composition (wt.%)	*y*	*a* (Å)	*c* (Å)	*c*/*a*	R-factor	Unit cell volume (Å^3)
Uncoated $LiCoO_2$	0.0	2.831	14.001	4.95	0.51	97.1
Mechano-thermal	0.3	2.845	13.914	4.89	0.63	97.5
$(100-y)LiCoO_2+$	1.0	2.838	13.828	4.87	0.48	96.5
$(y)TiO_2$	3.0	2.853	13.981	4.90	0.60	98.6
Sol–gel	0.3	2.832	13.921	4.92	0.54	96.6
$(100-y)LiCoO_2+$	1.0	2.821	13.862	4.91	0.49	95.5
$(y)TiO_2$	3.0	2.833	13.952	4.93	0.56	96.8

behavior of the coated samples were in agreement with this trend in the values of the *R*-factor.

3.2. Morphology

An SEM examination of the coated $LiCoO_2$ cathode materials shows that TiO_2 formed a uniform coating on the surface of the cathode particles, irrespective of the coating procedure. Fig. 3 compares the SEM images of the bare and 1.0 wt.% TiO_2-coated (mechano-thermal) $LiCoO_2$. The texture of the surface of the cathode particles appears distinctly changed upon coating. The increased brightness of the coated particles is due to the accumulation of charge on the non-conducting coating material as the electron beam impinges on it. Fig. 4 shows the HRTEM image of a 1.0 wt.% TiO_2-coated $LiCoO_2$ particle obtained by the mechano-thermal process. The coating material can be seen as a compactly-held kernel about 50 nm thick around the core cathode particle. Similar electron microscopic observations were made on coated materials obtained by the sol–gel process.

The BET surface area of the bare $LiCoO_2$ was 0.62 m^2/g. The surface areas of the 1.0 wt.% TiO_2-coated particles were 1.26 and 2.56 m^2/g, respectively, for the mechano-thermal and sol–gel processes. The larger surface areas of the coated materials are in accordance with the larger specific surface areas of the coating materials. TiO_2 used for the mechano-thermal process had a surface area of 50 ± 15 m^2/g. Therefore, an increase in the surface area of the cathode material by 0.64 m^2/g for the mechano-thermally coated material is commensurate with the 0.50 ± 0.15 m^2/g that can be obtained with a 1.0 wt.% coating of TiO_2.

3.3. ESCA

The spatial distributions of titanium, cobalt and oxygen in a 1 wt.% TiO_2 coated (mechano-thermal) sample are displayed in the depth profiles presented in Fig. 5a. The concentrations of titanium were too low compared to those of oxygen and cobalt. The depth profiles are highlighted in Fig. 5b. The concentration of cobalt increased up to a depth of about 40 nm and then leveled off. Similarly, it can be seen from Fig. 5b that the concentration of titanium dropped

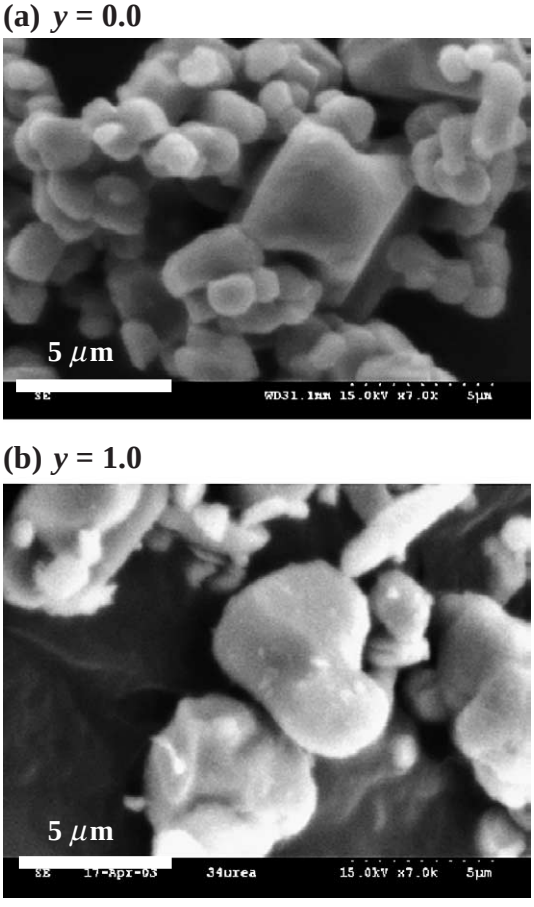

Fig. 3. SEM images of (a) the bare and (b) mechano-thermally coated $LiCoO_2$ (TiO_2-coating level: 1.0 wt.%).

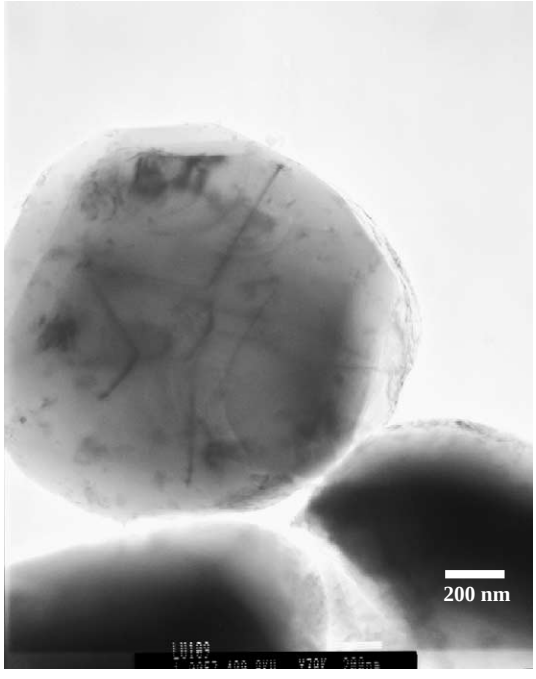

Fig. 4. HRTEM image of a 1.0 wt.% TiO_2-coated $LiCoO_2$ particle. Coating process: mechano-thermal.

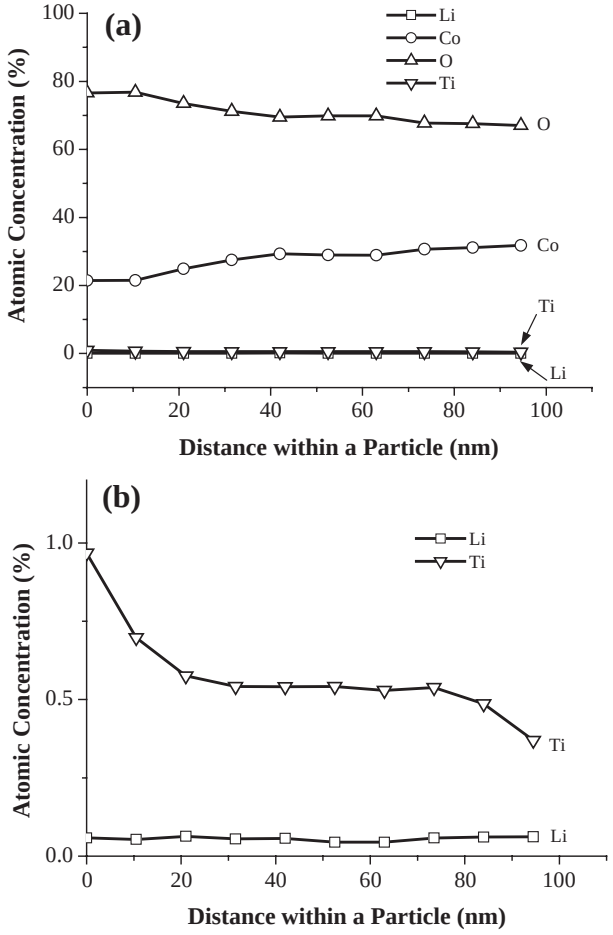

Fig. 5. (a) Depth profiles of titanium, cobalt and oxygen in a 1 wt.% TiO_2-coated $LiCoO_2$ sample. (b) Depth profile of titanium (expanded scale).

steeply up to about 40 nm. Thus, it appears that the cations in the coating material slowly diffused into the bulk of the cathode-active particle during the calcination process. This supposition is attested to by our XRD results, which suggested the formation of substitutional surface oxides.

3.4. Galvanostatic cycling

The effectiveness of the coatings obtained by the two processes in prolonging the cycle life of the cathode material was studied as a function of the TiO_2 coating level. Fig. 6 depicts the cycling performance of $LiCoO_2$ coated by the sol–gel process. The first-cycle discharge capacities of the materials were 169, 163, 160, and 156 mA h/g, respectively, for coating levels of 0.0, 0.3, 1.0 and 3.0 wt.%. The decrease in the capacity as the coating level was increased was due to the presence of inactive TiO_2 on the electrode.

The cycling data (Fig. 6) show that the coating improved the cyclability of the cathode material. We chose a cut-off value of 80 % for the capacity retention, calculated with the first-cycle discharge capacity of the respective material, to compare the number of cycles the cathode materials could sustain. Based on this cut-off regime, the bare $LiCoO_2$ could sustain just 12 cycles. The number of cycles rose to 46 for the material coated with 0.3 wt.% TiO_2. When the coating level was increased to 1.0 wt.%, the number of cycles jumped further to 64 cycles. Obviously, a coating level of 0.3 wt.% was beneficial, but could not result in a sufficiently compact coating. However, when the coating level was increased further to 3.0 wt.%, the cyclability fell. It is clear that at a coating level of 3.0 wt.%, the coating material led to a partial insulation of the cathode particles, lowering the capacity utilization and cyclability. The presence of excess coating material between the particles could also lower the particle-to-particle electronic conductivity, adversely affecting the coulombic efficiency. The *R*-factor determines the hexagonal ordering in the crystal structure: the lower the *R*-factor, the better the hexagonal ordering. The cyclability of

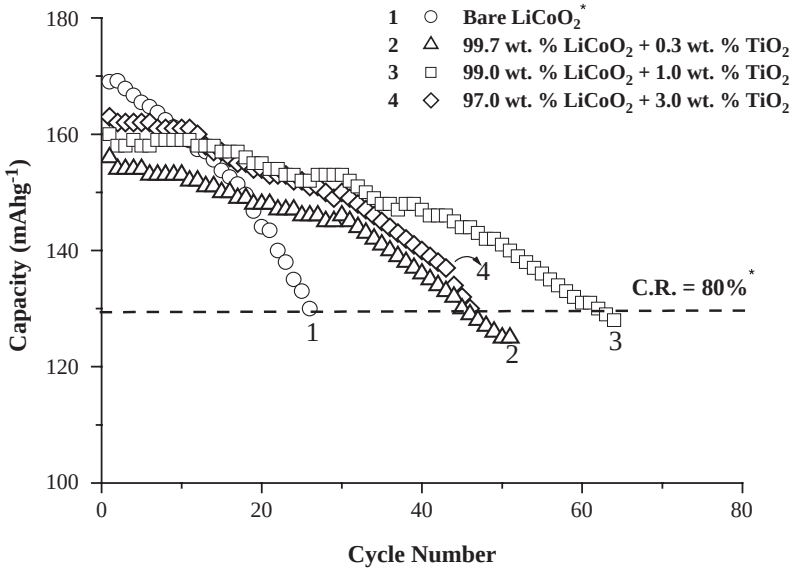

Fig. 6. Cycling performance of $LiCoO_2$ coated with TiO_2 by the sol–gel process. Charge–discharge: 2.75–4.40 V; 0.2 C rate.

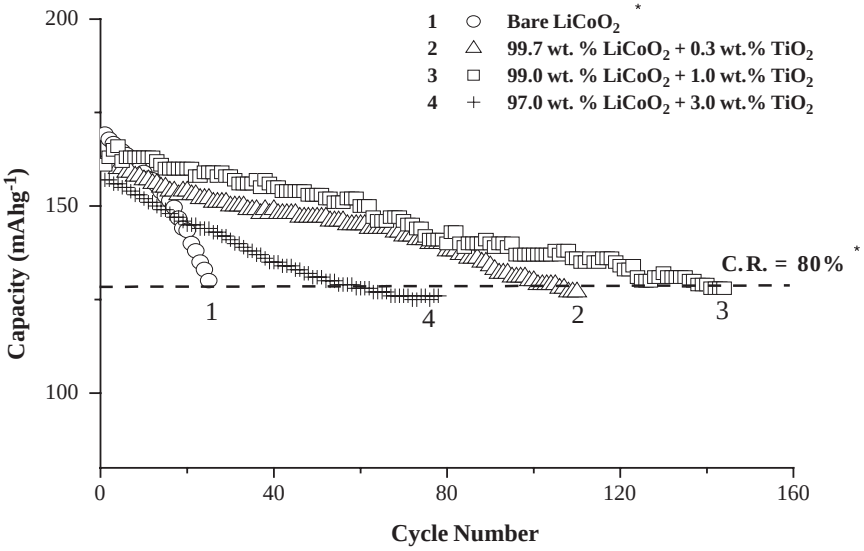

Fig. 7. Cycling performance of $LiCoO_2$ coated with TiO_2 by the mechano-thermal process. Charge–discharge: 2.75–4.40 V; 0.2 C rate.

the materials is roughly commensurate with the trend in the variation of the *R*-factor. It can be seen in Table 1 that the *R*-value was the lowest at the 1.0 wt.% coating level. According to Courtright [26], thinner coatings produce smaller cracks that are a factor in controlling the ingress of molecular species. It can be seen that at a 1.0 wt.% TiO_2 coating level, the cyclability of the cathode material registered a 5-fold improvement.

Fig. 7 depicts the cycling performance of the mechano-thermally coated samples. The first-cycle discharge capacities of the materials were 169, 161, 156 and 156 mA h/g, respectively, for coating levels of 0.0, 0.3, 1.0 and 3.0 wt.%. As with the sol–gel derived coatings, the mechano-thermal coatings also bestowed improved cycling characteristics on $LiCoO_2$. For a cut-off value of 80% capacity retention, the number of cycles that the materials sustained reached a maximum of 144 cycles for the material coated with 1.0 wt.% TiO_2. This represents a 12-fold improvement in cyclability. The superior performance of the 1.0 wt.% coated sample is in agreement with the lowest *R*-factor for this material.

Fig. 8 illustrates that at the optimal coating level of 1.0 wt.% TiO_2, the mechano-thermally coated material sustained a larger number of cycles than the sol–gel coated material. This suggests that the mechano-thermal coating process results in a material with better electrochemical

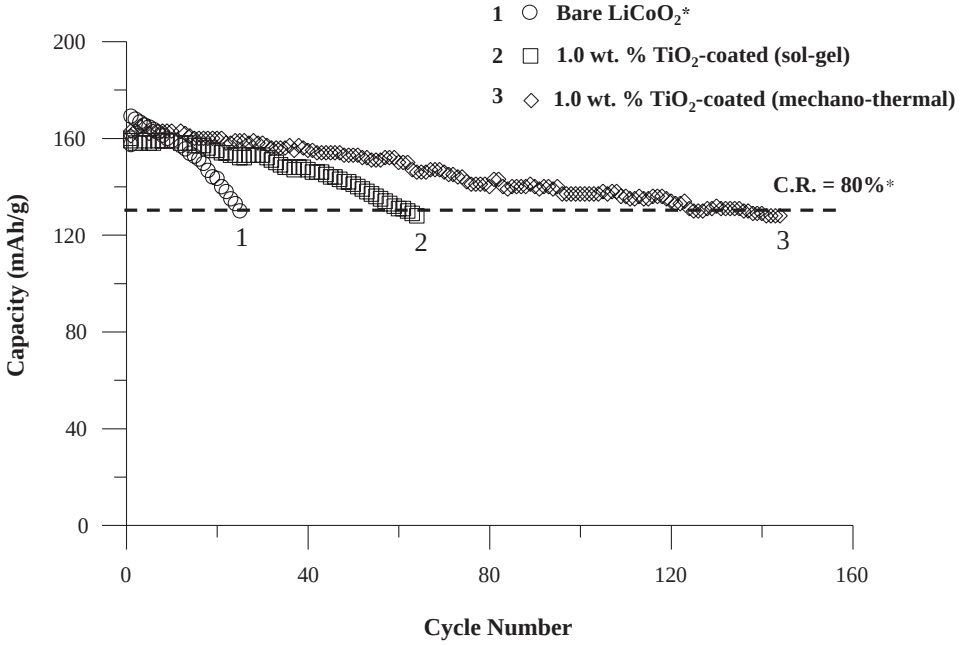

Fig. 8. Comparison of the cycling behavior of sol–gel-coated and mechano-thermally-coated $LiCoO_2$. TiO_2 coating level: 1.0 wt.%. Charge–discharge: 2.75–4.40 V; 0.2 C rate.

Table 2
Particle size and phase composition data on TiO_2 powders used for the mechano-thermal coating process

Sample	Particle size (nm)	Percentage	
		Anatase (%)	Rutile (%)
A	21.7	trace	99.9
B	35.0	31.3	68.7
C	21.5	8.3	91.7
D	5.0–20.0	65.1	34.9
Degussa	21.0	75.0	25.0

characteristics. Moreover, the mechano-thermal coating process is a simple, inexpensive and commercially viable one. These advantages must be weighed against the pitfalls of the sol–gel process which include the use of expensive alkoxide precursors like *sec*-butoxides and ethylhexanate diisopropoxides, generation of the green bodies in organic solvents like *iso*-propanol, and the release of environmentally hazardous solvent and alcoholic by-products during the evaporation and calcination processes. The mechano-thermal coating process can be an economic, convenient and clean alternative to the sol–gel coating process.

3.5. Effect of particle size and phase composition in the mechano-thermal coating process

Because the coating particles must adhere to the cathode surface and form a compact kernel, the particle size of the coating material should play an important part in deciding the film characteristics, and, therefore, the performance of the coated materials. With this in mind, several nano-particulate TiO_2 samples were tested as coating materials. Table 2 gives relevant data on the coating materials. Samples A, B, C and D were prepared by chemical vapor deposition and sourced from Yuan-Tse University (Taiwan). Available data on the samples are shown in Table 2. The coating levels were fixed at 1.0 wt.%. Fig. 9 depicts the cycling behavior of the various coated samples. Although one might expect that because the smallest particles would form the tightest assembly and yield the most compact film bestowing the best characteristics, our observations do not corroborate this reasoning. The performance of the coating is likely to be decided by such factors as size and shape of the particles, surface area, porosity, and even by the allotropic modification of the material. In fact, the rutile, anatase and brookite forms of TiO_2 have different electrochemical characteristics [27–30]. One conclusion that emerges from the study of the mechano-thermally coated materials is the probable superiority of the anatase form of TiO_2 over the rutile form. However, understanding how their electrochemical properties influence the behavior of the coatings calls for a separate study. The results indicate that because the electrochemical properties of the mechano-thermally coated materials are determined by the nature of the pre-formed coating particles, it is logical to conclude that mechano-thermal method is superior over sol–gel process.

3.6. Cyclic voltammetry

$LiCoO_2$ cathodes are known to undergo a hexagonal-monoclinic-hexagonal phase transition above 4.1 V vs. Li^+/Li, which leads to capacity fade upon repeated cycling [3,7,10]. This phase transition is accompanied by a 1.2% expansion of the lattice in the *c*-direction, which is considered to be above the limit of ~0.1% in elastic strain that oxides can tolerate [31]. The abrupt shrinkage of the *c*-

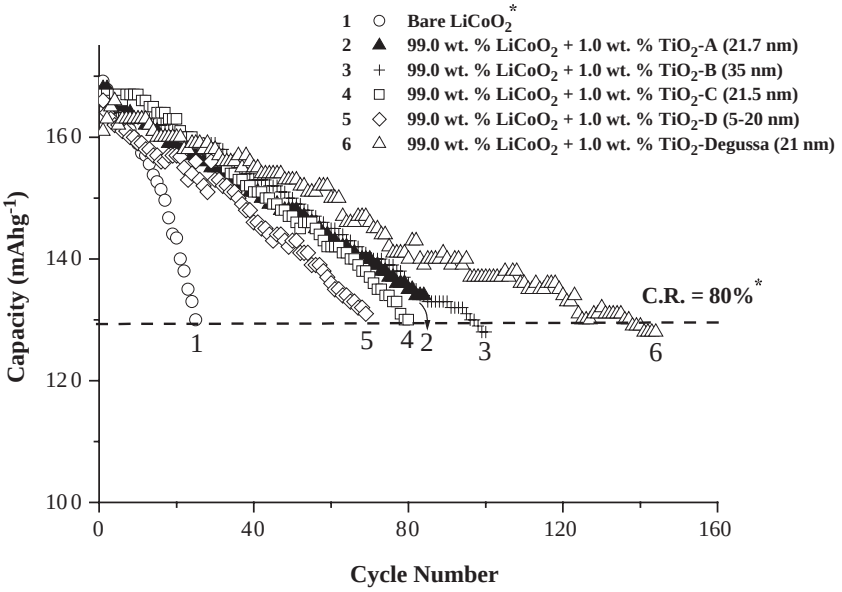

Fig. 9. Cycling performance of TiO_2-coated $LiCoO_2$ as a function of the particle size of TiO_2. Coating method: mechano-thermal process. Charge–discharge: 2.75–4.40 V; 0.2 C rate.

axis, which accounts for about 9% in volume change [32], can induce cracks in the particles, reducing the cyclability [3]. According to Kavan and Gratzel [33], cyclic voltammetry is sensitive to phase transformations occurring during electrochemical reactions. Thus, slow scan cyclic voltammetry was performed in order to examine the effect of the coating on the phase transitions that accompany the charge–discharge processes. Fig. 10a presents the cyclic voltammograms of the bare $LiCoO_2$, while Figs. 10b and c present those for $LiCoO_2$ coated by the sol–gel and mechano-thermal processes, respectively (TiO_2 coating level: 1.0 wt.%). Fig. 10a shows that the peaks corresponding to the phase transitions persist in every cycle. However, such peaks can be observed only in the first cycle for 1.0 wt.% coated materials (Fig. 10b and c). From the second cycle onwards, the peaks seem suppressed, which indicates that any defect in the coating that might have been present initially got repaired upon repeated cycling. The presence of cracks, pinholes, and other coating defects on coated surfaces is inevitable, but such defects may form and close

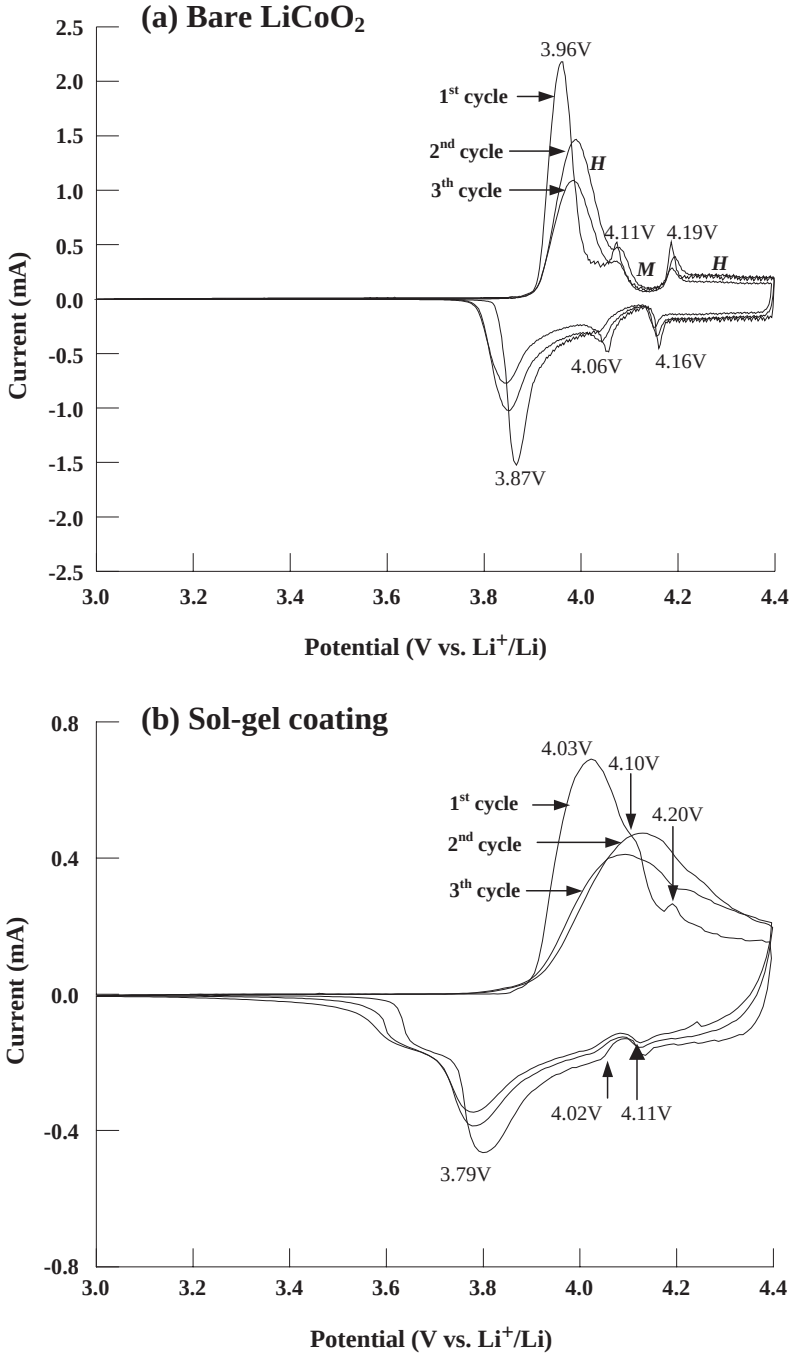

Fig. 10. Cyclic voltammograms of (a) bare $LiCoO_2$; (b) $LiCoO_2$ coated by the sol–gel method; and (c) $LiCoO_2$ coated by the mechano-thermal method. TiO_2 coating level: 1.0 wt.%. Voltage window: 3.0–4.4 V; scan rate: 0.025 mV/s.

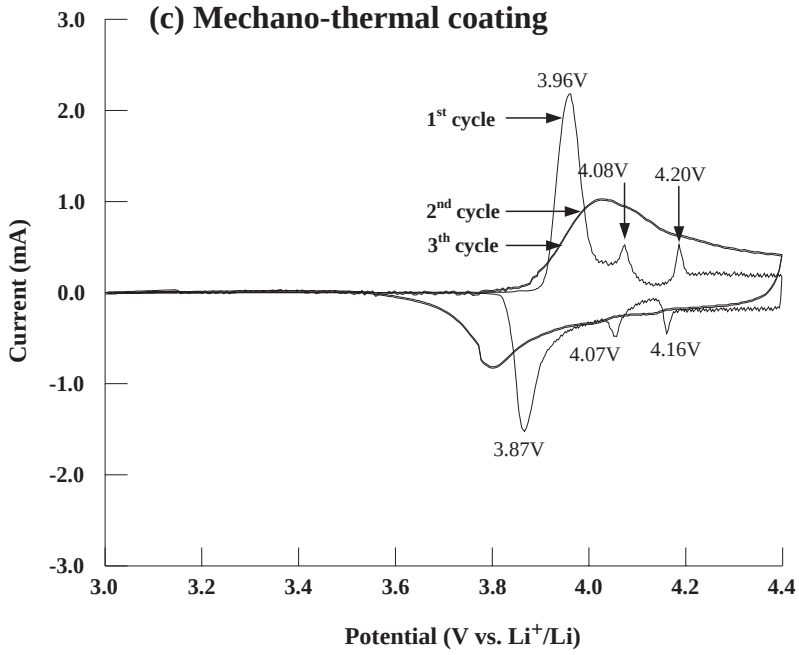

Fig. 10 (*continued*).

with the application of a load, or upon thermal cycling. Thus, as the lattice contracts and expands during the cycling processes, the surface texture of the active material particles changes, enabling the coating material to become ingrained in the crevices and cracks on the cathode surface. The more compact kernel that results leads to a suppression of the phase transitions, enhancing the cyclability of the coated material. In fact, the cyclic voltammograms of the coated materials (Fig. 10b and c) show little evidence for such transformations from the second cycle onwards even at 4.4 V vs. Li^+/Li. The absence of phase transitions in the coated samples ensures negligible strain, resulting in a longer cycle life.

4. Conclusions

Commercial $LiCoO_2$ samples were coated with TiO_2 by two processes: a sol–gel process from titanium tetrabutoxide and a mechano-thermal process from pre-formed TiO_2 nanoparticles. Although the XRD patterns of the coated materials did not show any extraneous peaks corresponding to the coated particles, the generally smaller values of the lattice parameter, c, of the coated samples suggested that substitutional compounds of the composition $Li_xTi_yCo_{1-y}O_{2+0.5y}$ might have formed on the surface of the cathode. Electron microscopic images of 1.0 wt.% TiO_2-coated particles revealed that the oxide formed a compact coating over the cathode particles. XRD studies showed a general decrease in the value of the lattice parameter c upon coating, indicating that substitutional compounds might have formed on the surface upon calcination. Galvanostatic charge–discharge studies suggested that a coating level of 1.0 wt.% was optimal for materials with good cycling characteristics. The lowest R-factor value for this material supports the good structural stability of the 1.0 wt.% coated sample, which confers the high cyclability. While the material obtained by the sol–gel coating procedure enhanced cyclability 5-fold, the one obtained by the mechano-thermal method delivered as much as a 12-fold improvement. Cyclic voltammetric studies showed that the coating led to a suppression of the cycle-limiting hexagonal/monoclinic/hexagonal phase transitions accompanying the charge–discharge processes. The mechano-thermal coating process derived materials were found to possess better cycling properties than the sol–gel derived materials. Nevertheless, the mechano-thermal coating process presents a simple, inexpensive, environmentally benign and commercially viable procedure for the production of $LiCoO_2$ cathode materials with enhanced cyclability.

Acknowledgements

Financial support for this work was provided by the National Science Council of the Republic of China under contract No. NSC-91-2622-E-008-006-CC3. TPK thanks the NSC for the award of a post-doctoral fellowship.

References

[1] J.N. Reimers, J.R. Dahn, J. Electrochem. Soc. 139 (1992) 2091.
[2] T. Ohzuku, A. Ueda, J. Electrochem. Soc. 141 (1994) 2972.
[3] H. Wang, Y.-I. Jang, B. Huang, D.R. Sadoway, Y.-M. Chiang, J. Electrochem. Soc. 146 (1999) 473.
[4] J. Cho, Y.J. Kim, B. Park, Chem. Mater. 12 (2000) 3788.

[5] J. Cho, Y.J. Kim, B. Park, J. Electrochem. Soc. 148 (2001) A1110.
[6] J. Cho, Y.J. Kim, T.-J. Kim, B. Park, Angew. Chem., Int. Ed. 40 (2001) 3367.
[7] E. Plichita, S. Slane, M. Uchiyama, M. Salomon, D. Chua, W.B. Ebner, H.W. Lin, J. Electrochem. Soc. 136 (1989) 1865.
[8] K. Mizushima, P.C. Jones, P.J. Wiseman, J.B. Goodenough, Mater. Res. Bull. 15 (1980) 783.
[9] J.B. Goodenough, K. Mizushima, T. Takeda, Jpn. J. Appl. Phys. 19 (1980) 305.
[10] G.G. Amatucci, J.M. Tarascon, L.C. Klein, Solid State Ionics 83 (1996) 167.
[11] D. Aurbach, K. Gamosky, B. Markovsky, G. Salitra, Y. Gofer, U. Heider, R. Oesten, M. Schmidt, J. Electrochem. Soc. 147 (2000) 1322.
[12] Z. Wang, C. Wu, L. Liu, F. Wu, F. Wu, L. Chen, X. Huang, J. Electrochem. Soc. 149 (2002) A466.
[13] J. Cho, Y.J. Kim, T.J. Kim, B. Park, Chem. Mater. 13 (2001) 18.
[14] A.M. Kannan, L. Rabenberg, A. Manthiram, Electrochem. Solid-State Lett. 6 (2003) A16.
[15] H.J. Kweon, S.J. Kim, D.G. Park, J. Power Sources 88 (2000) 255.
[16] M. Mladenov, R. Stoyanova, E. Zhecheva, S. Vassilev, Electrochem. Commun. 3 (2001) 410.
[17] J. Cho, C.-S. Kim, S.-I. Yoo, Electrochem. Solid-State Lett. 3 (2000) 362.
[18] X. Wang, L. Liu, L. Chen, X. Huang, Solid State Ionics 148 (2002) 335.
[19] G.T.K. Fey, H.Z. Yang, T. Prem Kumar, S.P. Naik, A.S.T. Chiang, D.C. Lee, J.R. Lin, J. Power Sources 132 (2004) 172.
[20] G.T.K. Fey, Z.X. Weng, J.G. Chen, C.Z. Lu, T. Prem Kumar, S.P. Naik, A.S.T. Chiang, unpublished results.
[21] G.T.K. Fey, Z.X. Weng, J.G. Chen, C.Z. Lu, T. Prem Kumar, S.P. Naik, A.S.T. Chiang, D.C. Lee, J.R. Lin, J. Appl. Electrochem. 34 (2004) 715.
[22] A. Bianco, M. Paci, R. Freer, J. Eur. Ceram. Soc. 18 (1998) 1235.
[23] J. Cho, G.B. Kim, H.S. Lim, C.-S. Kim, S.-I. Yoo, Electrochem. Solid-State Lett. 2 (1999) 607.
[24] J.N. Reimers, E. Rossen, C.D. Jones, J.R. Dahn, Solid State Ionics 61 (1993) 335.
[25] J.R. Dahn, U. von Sacken, C.A. Michal, Solid State Ionics 44 (1990) 87.
[26] E.L. Courtright, Surf. Coat. Technol. 68-69 (1994) 116.
[27] D.T. Cromer, K. Herrington, J. Am. Chem. Soc. 77 (1955) 4708.
[28] W.H. Baur, Acta Crystallogr. 14 (1961) 214.
[29] M.S. Whittingham, M.B. Dines, J. Electrochem. Soc. 124 (1977) 1387.
[30] R. Marchand, L. Brohan, M. Tournoux, Mater. Res. Bull. 15 (1980) 1129.
[31] L.H. van Vlack, Physical Ceramics for Engineers, Addison-Wesley Publishing, Reading, MA, 1964.
[32] K. Dokko, M. Nishizawa, S. Horikoshi, T. Itoh, M. Mohamedi, I. Uchida, Electrochem. Solid-State Lett. 3 (2000) 125.
[33] L. Kavan, M. Gratzel, Electrochem. Solid-State Lett. 5 (2002) A39.